Original Article

Dosimetric Evaluation of Semiflex Three-dimensional Chamber under Unflatten Beam in Comparison among Different Detectors

Kanakavel Kandasamy, E. James Jebaseelan Samuel
Department of Physics, School of Advanced Sciences, VIT University, Vellore, Tamil Nadu, India

Abstract

Purpose: The goal of this study is to investigate the dosimetric properties of a Semiflex three-dimensional (3D) chamber in an unflatten beam and compare its data from a small to a large field flattening filter-free (FFF) beam with different radiation detectors. **Methods:** The sensitivity, linearity, reproducibility, dose rate dependency, and energy dependence of a Semiflex 3D detector in flattening filter and filter-free beam were fully investigated. The minimum radiation observed field widths for all detectors were calculated using lateral electronic charged particle equilibrium to investigate dosimetric characteristics such as percentage depth doses (PDDs), profiles, and output factors (OPFs) for Semiflex 3D detector under 6FFF Beam. The Semiflex 3D measured data were compared to that of other detectors employed in this study. **Results:** The ion chamber has a dosage linearity deviation of +1.2% for <10 MU, a dose-rate dependency deviation of +0.5%, and significantly poorer sensitivity due to its small volume. There is a difference in field sizes between manufacturer specs and derived field sizes. The measured PDD, profiles, and OPFs of the Semiflex 3D chamber were within 1% of each other for all square field sizes set under linac for the 6FFF beam. **Conclusion:** It was discovered to be an appropriate detector for relative dose measurements for 6 FFF beams with higher dose rates for field sizes more than or equal to 3 cm × 3 cm.

Keywords: Comparison with diode, ion chamber, and microdiamond, percentage depth dose and profiles measurement in flattening filter-free beam, semi-flex three-dimensional chamber in flattening filter-free beam, sensitivity, linearity, dose rate dependency and energy dependency, volume averaging effect, and least field size

Received on: 02-09-2023 **Review completed on:** 22-02-2024 **Accepted on:** 22-02-2024 **Published on:** 30-03-2024

Introduction

Modern linear accelerators (Linac) include both a flattening filter (FF) and a FF-free (FFF) beam. Volumetric modulated arc therapy, stereotactic body radiation therapy (SBRT), and stereotactic radiosurgery (SRS), in particular, are being used to treat cancer patients with limited yet greater doses provided to destroy tumors. Beam characterization, such as absolute and relative dose assessments, is primarily and dosimetrically based on correct delivery. SBRT and SRS, on the other hand, are typically planned and delivered at linac machine using FFF beam. When the FF is removed, the beam intensity increases, especially toward the middle axis. Increased intensity reduces treatment time, particularly for high-dose stereotactic radiotherapy/SRS (SRT/SRS). As an added benefit, the FFF beam has a higher dose rate and a conical beam in shape due to the absence of a FF, resulting in a shorter treatment time and sparing normal tissues around cancer cells. For ion chambers of various sizes in measurements, two main effects were presented in FFF Beam: (1) ion recombination effects due to the higher dose per pulse in the absence of attenuation from the removed FF and (2) volume averaging in dose measurement due to the forward peaked bremsstrahlung of the unflattened beam.[1-4]

In general, detectors that were favored for measurements on ordinary flattened linac beams were either less suitable for FFF beams or required modifications.[5] A detector should also exhibit the following dosimetric characteristics: sensitivity, linearity, energy independence, reproducibility in measurement, minimal dose rate, and angular dependencies, as defined by the International Electrotechnical Commission (IEC-60731).[6] The detector shall meet the measurement conditions for determining percentage depth dose (PDD), profiles, and output

Access this article online

Quick Response Code:

Website: www.jmp.org.in

DOI: 10.4103/jmp.jmp_115_23

Address for correspondence: E. James Jebaseelan Samuel
Research Supervisor and Professor - Higher Academic Grade, Department of Physics, School of Advanced Sciences, VIT Vellore, Tamil Nadu, India.
E-mail: ejames@vit.ac.in

How to cite this article: Kandasamy K, Samuel EJ. Dosimetric evaluation of Semiflex three-dimensional chamber under unflatten beam in comparison among different detectors. J Med Phys 2024;49:84-94.

factors (OPFs) from the smallest to the largest field sizes set in a linac as specified by the International Atomic Energy Agency (IAEA) Technical Reports Series (TRS) 398 Standard and IEC 60976.[7,8] Due to source partial occlusion and a lack of lateral charged particle equilibrium (LCPE) in small field dosimetry, any radiation detector should have a minimum volume to produce a low volume averaging effect, according to IAEA TRS 483 code of practice.[9]

Commercially different ionization chambers (Semiflex, Semiflex three-dimensional [3D], and Microion chambers), different types of shielded and unshielded diodes, and special detectors – microdiamond are available in the industry for absolute and relative dose measurements. However, there is no ideal detector that satisfies all dosimetric properties from tiny to big fields. In case of diodes, despite their tiny dimensions and great sensitivity, diode detectors are not totally ideal due to their energy dependence at low energies and overresponse of shielded diodes (due to the high-Z shield).[10] However, for the ion chambers, because of the volume averaging effect and low air density, tiny volume ion chambers are less dependent on photon beam energy than diodes but are less appropriate for small field dosimetry.[11] Another option is a microdiamond detector, which has qualities such as radiation hardness, near-tissue equivalence, compact size, and independence from radiation quality. Ralston *et al*. achieved adequate penumbra measurement and reproducibility of the microdiamond results. However, research has shown that these detectors cannot achieve all of the small-field aspects and overrespond due to high density.[12-15]

A New Semiflex®3D (Modal: T31021) ionization chamber introduced by PTW Freiburg, Germany, which boasts an active volume of 0.07 cm^3 and near-water equivalence, energy independence, and a three-dimensional structure. In comparison with the previous version Semiflex 31010, the sensitive volume of the 31021 is designed with equal values of the length and the diameter to provide a negligible directional dependence of its response, hence the name Semiflex 3D. Hence, as an advantage, the orientation of the chamber can be both axial and radial direction for relative measurements.[16]

Momeni Harzanji *et al*. investigated the linearity, stability, angular dependence, temperature dependence, and relative dosimetry of PDD and profiles measuring up to 5 cm × 5 cm for 6X FF and 15 MV photon beam. The results of the Semiflex 3D chamber were evaluated exclusively using a microdiamond detector.[17] Casar *et al*. conducted an investigation into the dosimetric outcomes of different detectors, including the Semiflex 3D detector, specifically for 6FF and 6FFF beams. However, their analysis was limited to field widths spanning from 0.6 cm × 0.6 cm to 10 cm × 10. The authors also provided OPFs and correction factors in adherence to TRS 483.[18] A comprehensive study regarding the dosimetric characteristics of Semiflex 3D in unflattened beam with high-dose rate and performance comparison among different detectors was not been attempted.

This study's objective is to study dosimetric characteristics such as sensitivity, linearity, reproducibility, dose rate dependency, energy dependency, PDD, profiles, and OPF for a Semiflex 3D chamber and compare those parameters with four distinct detectors operating under FFF beam in accordance with IAEA TRS 483, IEC 60731, and Atomic Energy Regulatory Board (AERB) Standards.

Materials

A linear accelerator (Infinity–Model) from (Elekta, Sweden) was utilized for this inquiry. In addition to 6X FFF photon beam energies, the machine features 10X, 15X, and 6X FF beam energies. At 600 MU/min and 1600 MU/min, maximum dose rates were observed for FF and FFF energies, respectively.[19] The PTW detectors:[20] Semiflex 3D (SF3D), Pinpoint, Diode P, and Microdiamond, which are detailed in Table 1, were employed to obtain measurements using the MP3-M 3D Water Phantom under the linac.[21] A pictorial representation is given for the mentioned detectors as below in Figure 1.

Methods

International Electrotechnical Commission performance evaluations

IEC 60731 actually recommends standard tests and tolerances for dosimetric characteristics of a measuring assembly, i.e., an ionization chamber. A conventional phantom setup comprising a 10 cm depth, 100 cm source-to-surface distance (SSD), and 10 cm × 10 cm field area was employed in the linac to ascertain the following characteristics: sensitivity, linearity, reproducibility, energy dependence, and dose rate dependency. A comparison of the aforementioned generic dosimetric characteristics according to IEC 60731 and manufacturer specifications for a SF3D Chamber is presented in Table 2.

Sensitivity and linearity

Monitor units (MUs) of 5, 10, 20, 30, 50, 100, 200, 300, and 500 were chosen, and meter readings for sensitivity and linearity were taken for 6FFF beam. Two approaches were employed to determine the sensitivity of the detectors used in this study. For each

MU, the ratio of meter reading to delivered MU was first examined. The average ratio was determined for each detector to allow for response intervariation, and a graph was created between the average ratio and the detectors directly, yielding sensitivity due to detector volume and medium. Second, the Semiflex Chamber ratio was used to standardize the ratios of all MUs in each detector. At small MUs, this impacts the sensitivity of each detector. Linearity error is determined by the ratio of MUs and meter readings; a graph was generated between MU versus ratio for each detector.[22]

Reproducibility

The reproducibility test was performed on low and standard MU, i.e., 10 and 100 MU, and meter readings were taken ten times for 6FFF beam. Among those readings, the percentage deviation was determined.[22]

Table 1: Basic characteristics of radiation detectors used in this work are tabulated

Detectors (modal)	Type of detector	Nominal characteristics of radiation detectors				
		FS (cm^2)	Volume (mm^3)	Detector orientation	Reference point of measurement	Nominal voltage (V)
SF3D-31021	Air ionization chamber	2.5…40	70	Radial*	Central axis at water surface	400
Semiflex 31010	Air ionization chamber	3…40	125	Radial	Central axis at water surface	400
Pinpoint 31014	Air ionization chamber	2…30	15	Radial	Central axis at water surface	400
MD-60019	Carbon synthetic diamond	1…40	0.004	Axial	On detector axis, 1 mm from detector tip, marked by ring	0
Diode P 60016	Silicon shielded diode	1…40	0.03	Axial	On detector axis, 2.42 mm from detector tip	0

*As per the manufacturer, SF3D can also be positioned at axial orientation. The chamber was positioned at radial orientation throughout the measurements for inter comparison. MD: Microdiamond, SF3D: Semiflex 3D, FS: Field Size

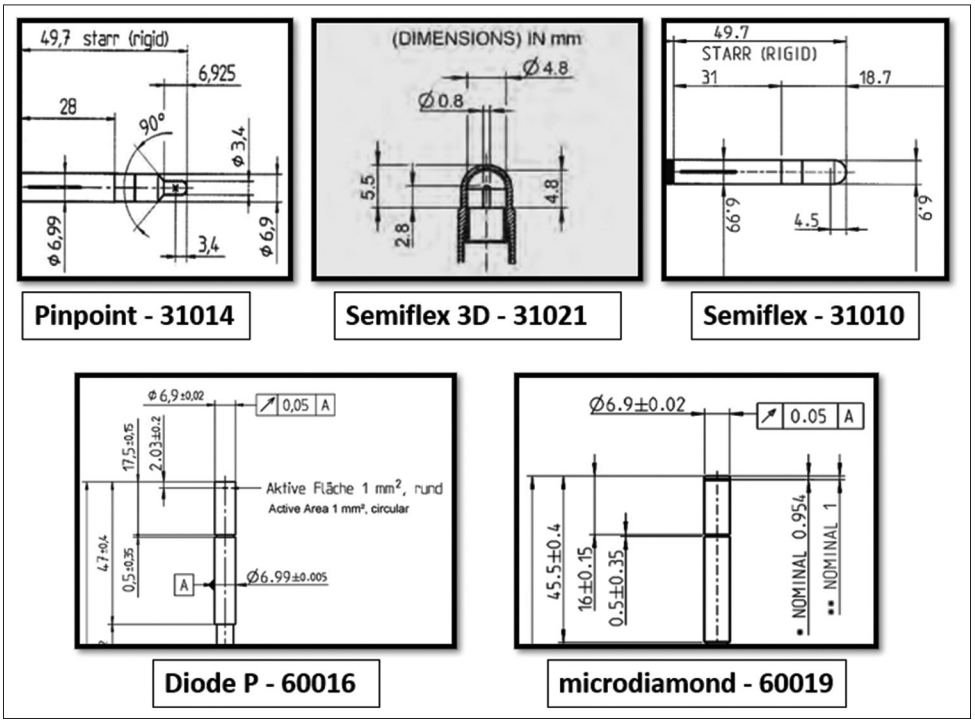

Figure 1: A schematic diagrams of each detector used in this study

Dose rate dependency

The dose rate was modified in the linac (service mode) to 200, 400, 600, 800, 1000, 1200, and 1600 MU/min under 6FFF Photon Beam, and the appropriate meter reading was recorded. Because silicon is more dependent on dose rate, a Diode *P* Detector was not used in this Dose Rate experiment.[23]

Energy dependence

Photon beam energies of X6, X6FFF, X10, and X15 MV were employed for energy dependency verification. The beam quality index was measured for each energy for each detector using the MP3M system and standardized to the machine's standard Beam Quality Index provided by the manufacturer.[7]

Detector field size determination

In accordance with IAEA TRS 483, it was decided to identify the smallest measuring field size for each detector before using them for relative measurements. The IAEA TRS 483 Protocol[9] formulas were used to compute the range of LCPE (rLCPE) and full-width half maximum (FWHM).

$$r_{LCPE} = 8.369 \text{ X } TPR_{20/10}(10) - 4.382 \quad \text{----------(1)}$$

$$FWHM > 2r_{LCPE} + d \quad \text{----------(2)}$$

where

$TPR_{20/10}(10)$ is the beam quality index for a 10 cm × 10 cm field size measured in a 6FFF beam.

d is the size of the detector (the greatest distance between two spots on the detector's outside edge).

$TPR_{20/10}$ was practically measured for the 6FFF beam using all of the aforementioned detectors and used to compute rLCPE, with the accompanying FWHM calculated using the formula.[2] The predicted field size and manufacturer parameters are shown in Table 3.

Relative dosimetry performance

To examine the SF3D ion chamber's performance in relative dosimetry, 6 MV FFF photon beam quality and field sizes of (3, 5, 10, 20, and 30) cm^2 were used, with microdiamond (MD) used as the reference detector. The minimal field size, as defined in Table 3, was employed in this case. Measuring detector sensitivity due to thermal equilibrium, stability, and applied bias voltage was done carefully for the best detector performance. PDDs, profiles, and OPFs were evaluated using Semiflex 3D and other detectors. For all PDD and profile measurements and detectors, the water scanning system was set to step-by-step scanning mode, 1 mm step size, and an 8 mm/s speed.

Percentage depth dose

When calculating the PDD of high-energy photon beams using a cylindrical ion chamber, the effective point of measurement, reff = $0.6r_{cav}$, was used, where r_{cav} is the radius of the relevant cylindrical ionization chamber according to IAEA TRS 398 Standard. The Diode P and MD detectors, on the other hand, were installed at their respective reference points of measurement to be matched with the SSD according to the vendor's specifications. The PDDs of all detectors (ranging from 0 to 250 mm deep) were measured. To define and identify each detector's performance, PDD curves were normalized to central axis maximum dose for each field size, and metrics parameters $PDD_{50\ mm}$, $PDD_{100\ mm}$, $PDD_{200\ mm}$, and $PDD_{230\ mm}$ were obtained from each PDD curve of each detector for each field size. Depths in millimeters were denoted by 50, 100, 200, and 230. These parameters were converted to MD data, and a graphical representation was made. For each field size, the aforementioned metrics were calculated and graphically contrasted. Areas under the maximum limit depth of dosage and shallow depths that were not considered for dose assessment usually have a high level of uncertainty at the build-up region.[24]

Table 2: Dosimetric properties and its variation for a chamber

Description	IEC 60731 limits	Manufacturer limits
Sensitivity	Not mentioned	
Reproducibility	+0.5%	≤ ±0.3%
Dose rate dependency	+0.5%	≤ ±0.5%
Energy dependency	+2% under C-60–25 MV photon	
Linearity	+1%	Not mentioned

IEC: International Electrotechnical Commission

Radial profiles

Profiles were created using 90 cm SSD and at 10 cm depth. Only inline profile measurements along the radial direction of the SF3D chamber were used for the abovementioned field widths and detectors because chamber axial direction (cross-line profile) will have a larger volume averaging impact, resulting in wider penumbra for different chambers. This is the case for Semiflex and Pinpoint. Two variables from each profile were used to compare detectors: field size and radiation penumbra. The average penumbra was calculated from the left and right penumbra, and the FWHM is defined as the location of the FFF beam's inflection point (IP). The AERB has developed a method for analyzing FFF beam profile. Field size was determined through IP analysis, which is implemented in the PTW Beamscan Software. For measured locations, this software computes the IP of an unflattened profile using the first-order derivative technique. In the case of penumbra, the dose value at the IP shall be used as the reference dose value (RDV). Points Pa and Pb, located at 1.6 and 0.4 times RDV, respectively, must be identified. The penumbra is defined as the lateral spacing between Pa and Pb on either side of the profile as shown in Figure 2.[25,26] Measured penumbra and field sizes of MD detector used as a reference.

Output factor

OPF was built with 90 cm SSD and at 10 cm depth. Calibrated Unidos E electrometer (PTW Freiburg) measurements were conducted for all of the radiation detectors indicated. The MD OPFs were considered the reference detector and were normalized to it.

Results

International Electrotechnical Commission performance evaluations

The Semiflex 3D chamber's sensitivity was investigated utilizing sensitivity coefficient calculations for the various MUs delivered for the 6FFF beam, normalized to the Semiflex Chamber (the standard ion chamber having the largest volume among those detectors). Figure 3a clearly displays how the SF3D chamber's sensitivity is performed among them. The SF3D chamber is roughly 30% less sensitive than a standard Semiflex chamber. For very low MU (5 MU), SF3D outperforms Semiflex by 0.6%, as seen graphically in Figure 3b.

The linearity and coefficient of the SF3D chamber were fitted using coefficient estimates for various progressive

Table 3: Deduced least full width half maximum of each detector as per TRS 483 method

Detector	r_{LCPE} (mm)	*d* – detector's maximum size (mm)	Manufacturer's least FWHM (cm)	Least FWHM as per TRS 483 (cm)
SF3D	12.478	5.855	2.5	3.00
Semiflex	12.294	16.365	3.0	4.00
Pinpoint	12.436	5.528	2.0	3.00
Diode P	12.126	4.423	1.0	3.00
MD	12.168	2.000	1.0	2.50

SF3D: Semiflex 3D, MD: Microdiamond, FWHM: Full width half maximum, TRS: Technical Series Reports

MUs delivered for the 6FFF beam normalized to 100 MU. Figure 4a and b exhibits the SF3D chamber's linearity behavior in contrast to other detectors. The SF3D chamber had the highest variation at 5 MU, which was 1.3%. A similar trend was observed in the pinpoint chamber.

The reproducibility of SF3D with different detectors at low (10 MU) and standard (100 MU) resolutions is shown in Figure 5. Almost all detectors demonstrated exceptionally good agreement in dose reproducibility for 100 MU dosage.

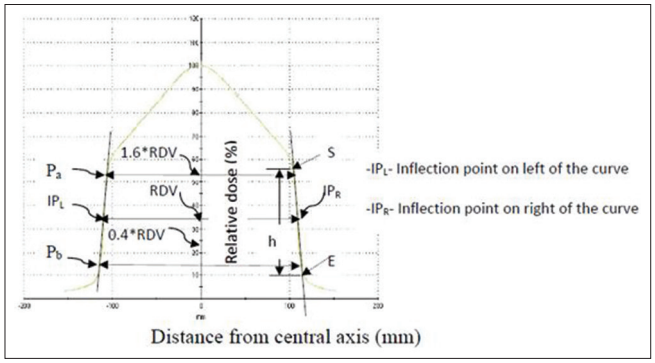

Figure 2: Schematic diagram for determining inflection point penumbra. RDV: Reference dose value

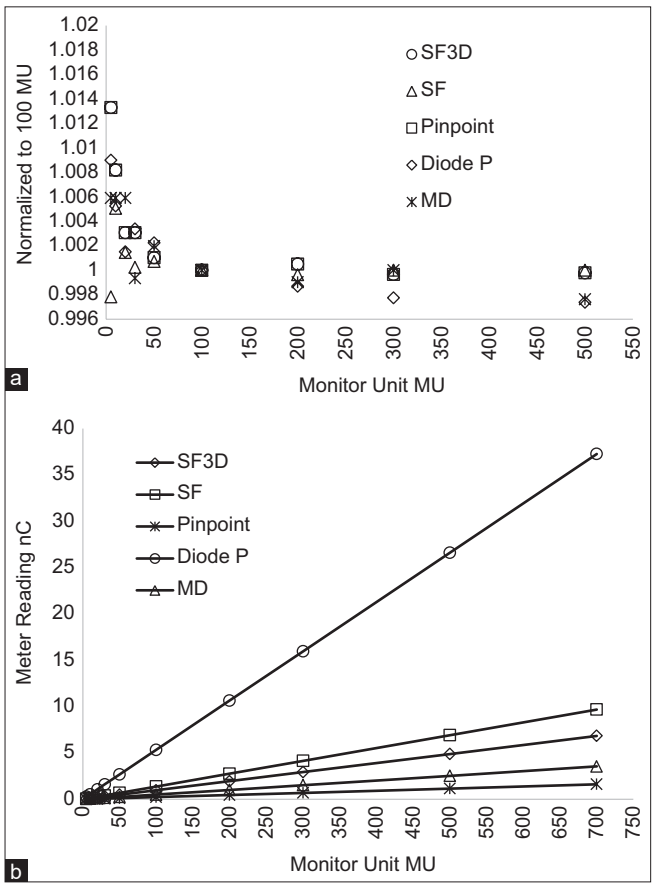

Figure 4: (a and b) Shows how detectors linearly behave varying from 5 to 500 monitor units. SF3D: Semiflex 3D, SF: Semiflex, FFF: Flattening filter free, MD: Microdiamond

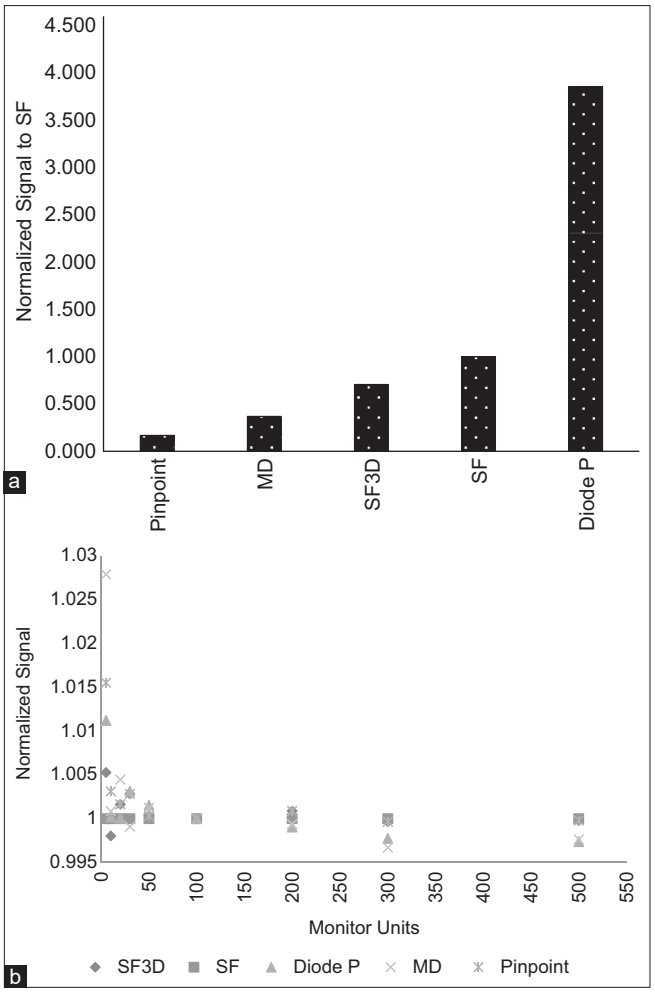

Figure 3: (a) Sensitivity of detectors and position of Semiflex three-dimensional chamber among them for 6 flattening filter-free beam. (b) Variation of sensitivity against monitor units for 6 flattening filter free beam, SF3D: Semiflex 3D, SF: Semiflex, FFF: Flattening filter free, MD: Microdiamond

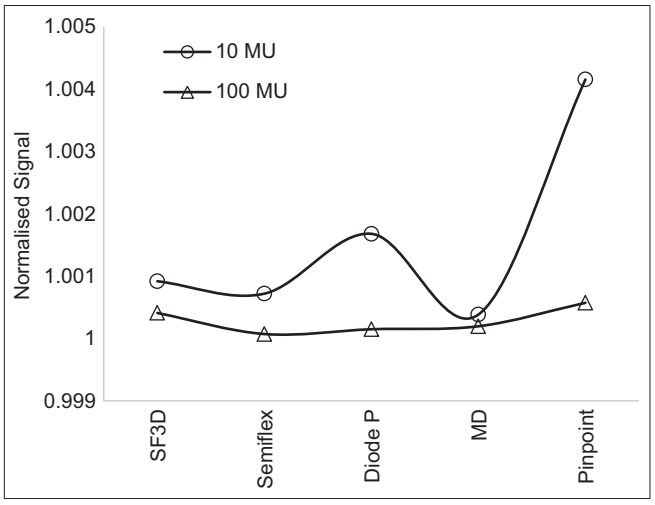

Figure 5: Reproducibility of radiation detectors for 10 monitor unit (MU) and 100 MU under 6 flattening filter-free beam. SF3D: Semiflex 3D, FFF: Flattening filter free, MD: Microdiamond

For 10 MU, the maximum variation for SF3D was 0.2%, and for Pinpoint, it was 0.5%.

All meter results at all exposure rates were standardized to the nominal dose rate (600 MU/min) for each detector for the dose rate experiment. Figure 6 displays the detectors' dose rate dependency. With the exception of the SF3D and pinpoint chambers, MD and Semiflex performed well from low-to-very high dose rates with no discernible percentage change. Both the SF3D and pinpoint chambers exhibited a slightly higher deviation (0.5%) for dosage rates >1000MU/min than the other two detectors.

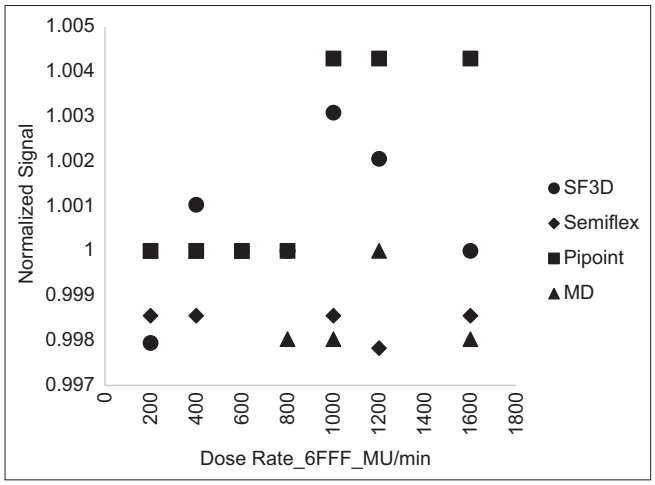

Figure 6: Dose rate dependency of radiation detectors for given dose rate under 6 flattening filter-free beam. SF3D: Semiflex 3D, MD: Microdiamond

Table 4: Maximum Deviation of Energy Dependencies

	Output factor				
	SF3D	Semiflex	Pinpoint	Diode P	MD
% Deviation	0.6352	0.9601	1.2340	1.0909	0.9509

SF3D: Semiflex 3D, FFF: Flattening filter free, MD: Microdiamond

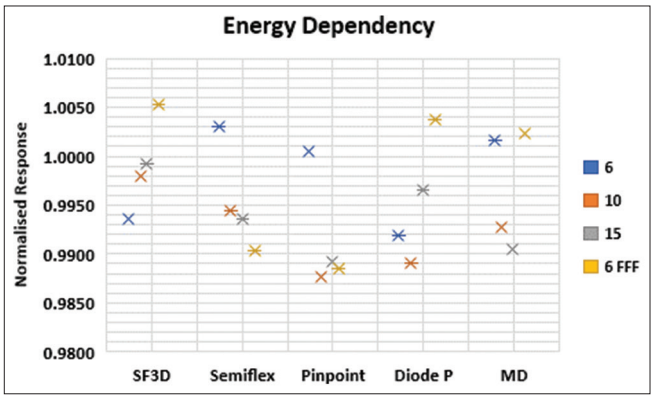

Figure 7: Energy dependency of detectors for photon beam including 6 flattening filter-free beam. SF3D: Semiflex 3D, FFF: Flattening filter free, MD: Microdiamond

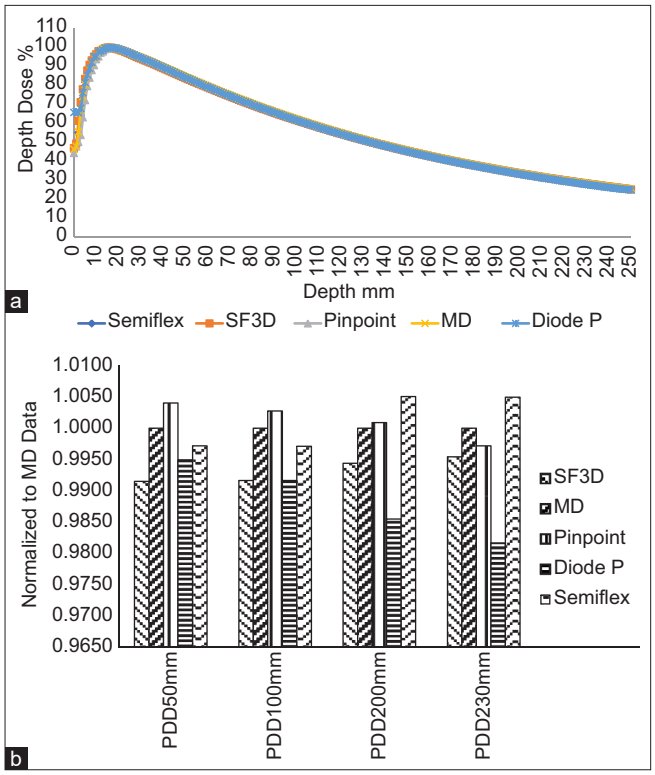

Figure 8: (a) Percentage depth dose curves of detectors for 3 cm × 3 cm FS. (b) Percentage depth dose metrics of detectors normalized to micro diamond for 3 cm × 3 cm. SF3D: Semiflex 3D, FFF: Flattening filter free, MD: Microdiamond, PDD: Percentage depth dose

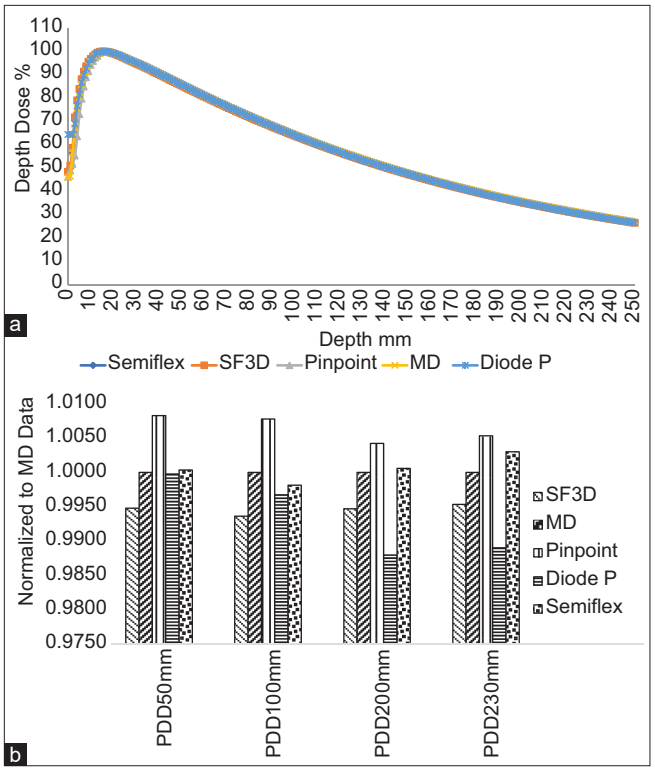

Figure 9: (a) Percentage depth dose curves of detectors for 5 cm × 5 cm FS. (b) Percentage depth dose metrics of detectors normalized to micro diamond for 5 cm × 5 cm. SF3D: Semiflex 3D, FFF: Flattening filter free, MD: Microdiamond, PDD: Percentage depth dose

The energy dependency test was used to determine and standardize the response of all detectors to different energies of photon beams. Figure 7 and Table 4 show the ionization chamber's energy versus response plot, as well as the highest divergence among detectors.

Depth dose

Figures 8a-12a show measured PDD curves. The parameters $PDD_{50\,mm}$, $PDD_{100\,mm}$, $PDD_{200\,mm}$, and $PDD_{230\,mm}$ were extracted, and deviations were noticed from each PDD curve of each detector. Metrics are graphically represented in Figures 8b-12b. Figure 13 and Table 5 show normalized SF3D to MD detector metrics against each field size and measured SF3D data for each field. When compared to MD, SF3D has a maximum percentage deviation of 0.9% for $PDD_{50\,mm}$ 3 cm × 3 cm field size. In $PDD_{230\,mm}$ of 30 cm × 30 cm, Diode P beats all other detectors.

Radial profiles

The FFF protocol-AERB was used to determine the radiation penumbra and FWHM. It is discovered that the SF3D chamber has a greater penumbra than the MD chamber. Semiflex Chamber produced the greatest penumbra. Figures 14-18 depicted measured profiles. Tables 6 and 7 show the measured FWHM and penumbra.

Output factor

All detector meter readings were recorded, normalized to 10 cm × 10 cm field size, and presented in Table 8. The appropriate graph for all OPFs is depicted in Figure 19. The MD's relative normalized OPFs were compared to those of other detectors in Figure 20.

Table 5: Semiflex 3D's percentage depth dose metrics data with respect to different square field sizes

Metrices	FS (cm)				
	3	5	10	20	30
$PDD_{50\,mm}$	83.89	85.36	87.15	87.59	87.58
$PDD_{100\,mm}$	61.64	63.83	67.06	69.17	69.63
$PDD_{200\,mm}$	33.53	35.48	38.72	41.75	42.64
$PDD_{230\,mm}$	28.19	29.85	32.86	35.77	36.74

PDD: Percentage depth dose, FS: Field size

Table 6: Measured field sizes from 3 cm to 30 cm for different detectors

FS (cm)	MD	Diode P	Pinpoint	SF3D	Semiflex
3	3.06	3.03	3.07	3.06	3.07
5	5.10	5.04	5.09	5.12	5.02
10	10.06	10.06	10.08	10.11	10.04
20	20.10	20.12	20.11	20.13	20.14
30	30.14	30.11	30.13	30.19	30.16

MD: Microdiamond, SF3D: Semiflex 3D, FS: Field size

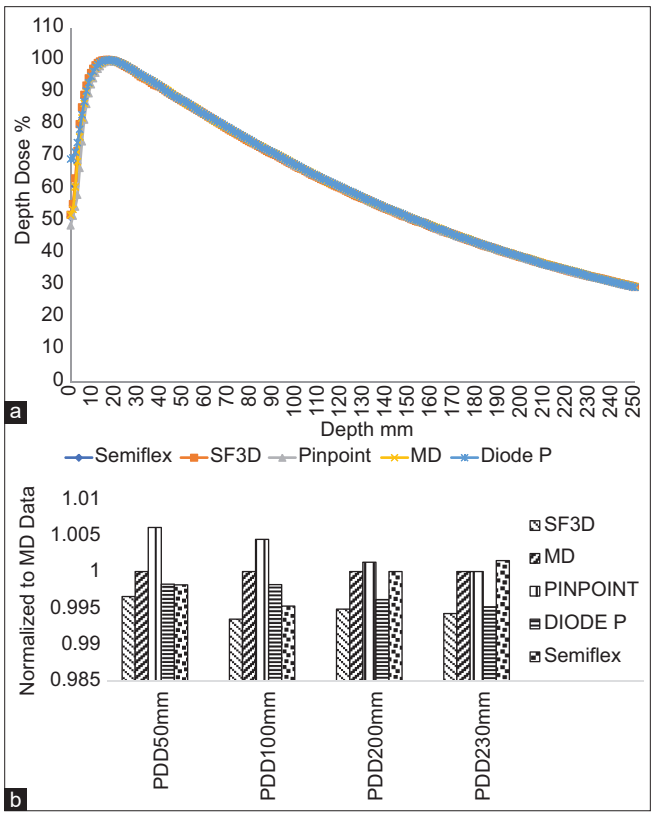

Figure 10: (a) Percentage depth dose curves of detectors for 10 cm × 10 cm FS. (b) Percentage depth dose metrics of detectors normalized to micro diamond for 10 cm × 10 cm. SF3D: Semiflex 3D, FFF: Flattening filter free, MD: Microdiamond, PDD: Percentage depth dose

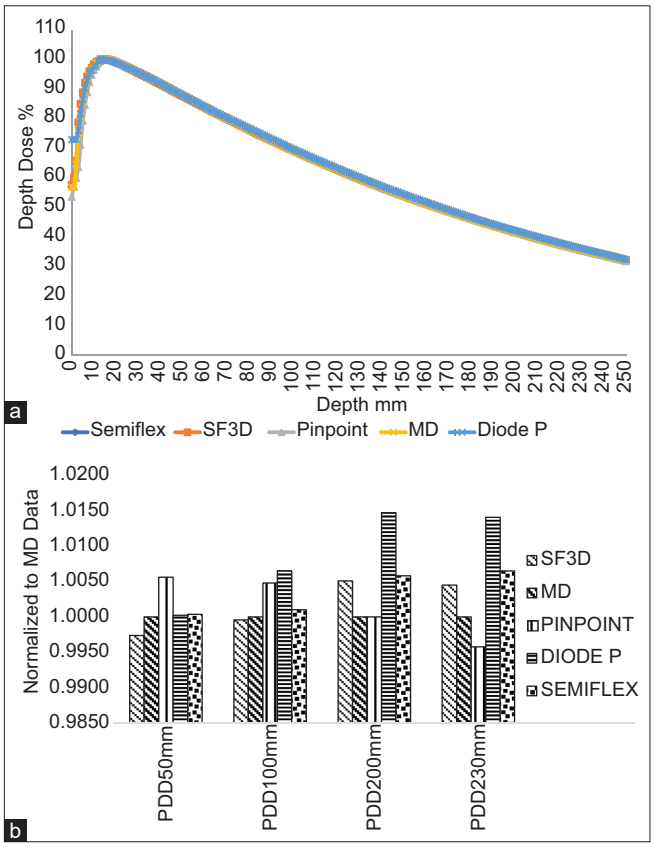

Figure 11: (a) Percentage depth dose curves of detectors for 20 cm × 20 cm FS. (b) Percentage depth dose metrics of detectors normalized to micro diamond for 20 cm × 20 cm. SF3D: Semiflex 3D, FFF: Flattening filter free, MD: Microdiamond, PDD: Percentage depth dose

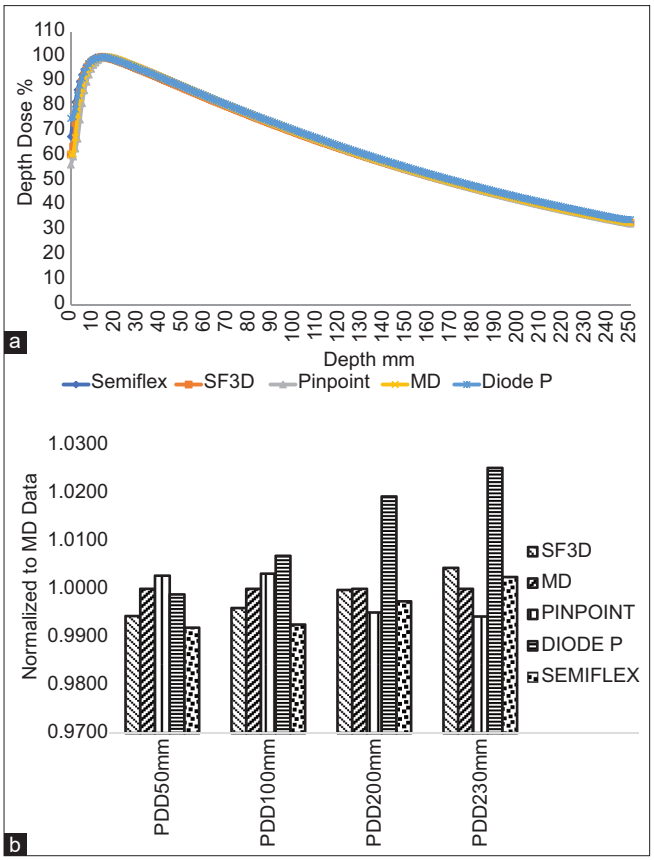

Figure 12: (a) Percentage depth dose curves of detectors for 30 cm × 30 cm FS. (b) Percentage depth dose metrics of detectors normalized to micro diamond for 30 cm × 30 cm. SF3D: Semiflex 3D, PDD: Percentage depth dose, MD: Microdiamond

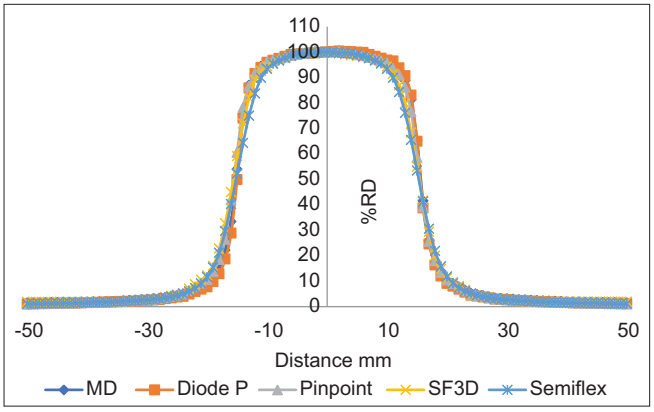

Figure 14: Radial profile curves are shown for 3 cm × 3 cm for different detectors. F3D: Semiflex 3D, MD: Microdiamond

Discussion

When the sensitivity of the SF3D is compared to that of other conventional detectors, it is observed that sensitivity changes depending on sensitive volume, atomic number, and medium. Figure 1a clearly indicates how the sensitivity of the SF3D chamber is distributed among them in terms of detector volume, medium, and medium Density. Due to its smaller

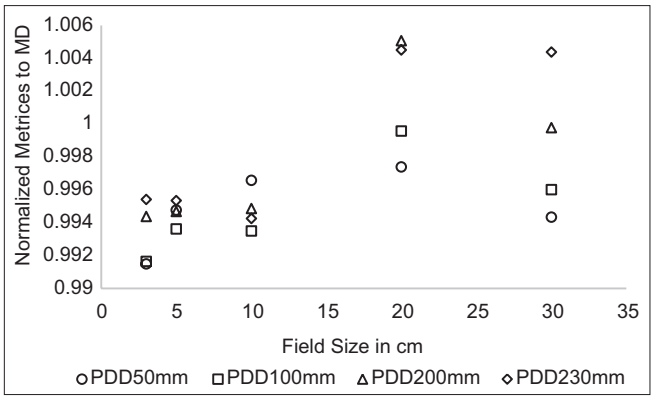

Figure 13: Normalized metrics of Semiflex three-dimensional chamber to microdiamond detector. SF3D: Semiflex 3D, PDD: Percentage depth dose

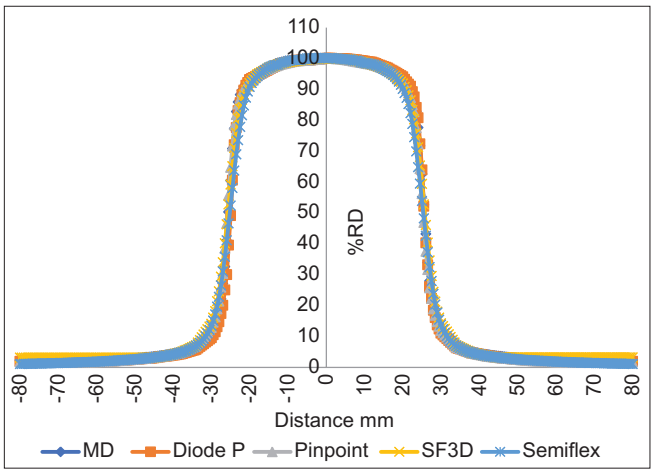

Figure 15: Radial profile curves are shown for 5 cm × 5 cm for different detectors. SF3D: Semiflex 3D, MD: Microdiamond

Table 7: Measured penumbra of different detectors against different field sizes

	Penumbra (mm) versus FS (cm)				
	3	5	10	20	30
MD	3.68	4.245	6.5	7	7.5
Diode P	3.39	3.75	6	6	8
Pinpoint	4.06	4.54	7	7.5	8
SF3D	5.13	5.66	8	8	9
Semiflex	5.695	6.315	8.5	9	10.5

MD: Microdiamond, SF3D: Semiflex 3D, FS: Field size

volume than a typical Semiflex chamber, the SF3D chamber has a 30% lower sensitivity. Due to its somewhat larger volume, SF3D has more sensitivity than MD and Pinpoint chamber. Diode P, on the other hand, has a very high sensitivity due to the density of the medium. This hypersensitivity is due to the silicon material and density of the Diode P (Density: 2.33 g/cm^3, atomic number: 14), and it is more sensitive to lower energy scatter photons.[26] Due to reduced volume, the SF3D chamber revealed a 0.5% variance with variable MU for <50MU dose when compared to the Semiflex chamber.

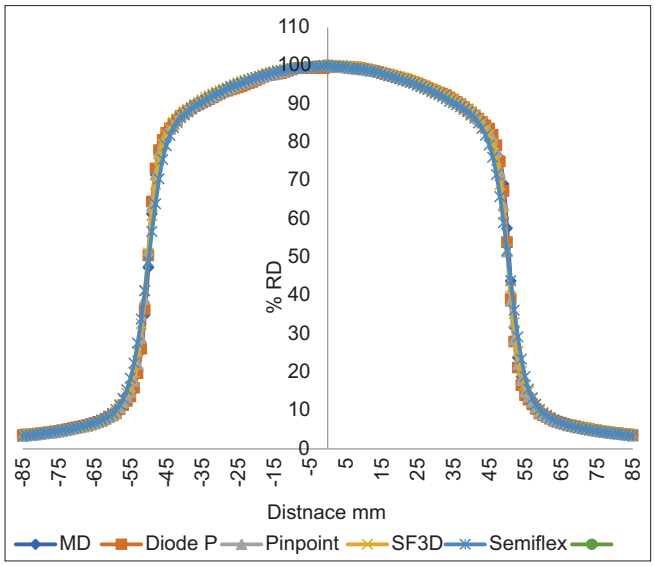

Figure 16: Radial profile curves are shown for 10 cm × 10 cm for different detectors. SF3D: Semiflex 3D, MD: Microdiamond

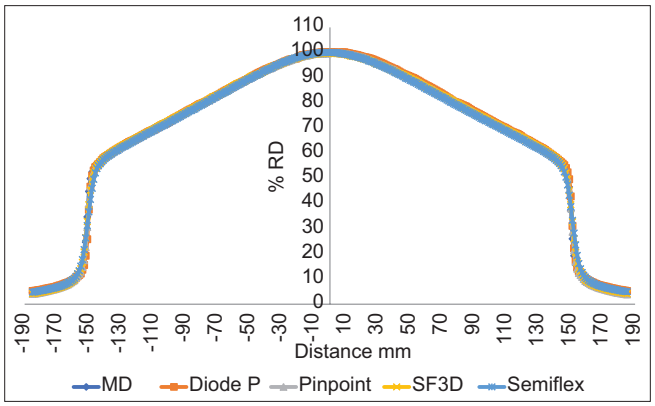

Figure 18: Radial profile curves are shown for 30 cm × 30 cm for different detectors. SF3D: Semiflex 3D, MD: Microdiamond

Figure 2a and b show that the largest deviations in linearity occur in low MU due to detector sensitivity.[27] The lower the volume of the ion chambers, the greater the divergence in linearity, particularly for low MUs. For the reproducibility test, all detectors performed well within 0.5%.[6] The largest variance was found to be 0.3% when comparing the SF3D chamber to other detectors in dose rate dependency. In the pinpoint chamber, the deviation was greater. This is due to the ion recombination and density perturbation effect, with greater dosage rates causing the most deviation.[7] Momeni Harzanji *et al*. already investigated SF3D for standard X6 Photon beam linearity and reproducibility. Our results for the X6FFF Photon beam were well within limitations and matched the previous studies.[17] In comparision to other detectors, the energy dependency was shown to be the lowest.[6] When compared to other detectors, the SF3D chamber had the biggest fluctuation in PDD at 0.8%. The MD, Semiflex, and pinpoint chambers all agree with it extremely well. In comparison to Diode P, $PDD_{200\ mm}$ and $PDD_{230\ mm}$

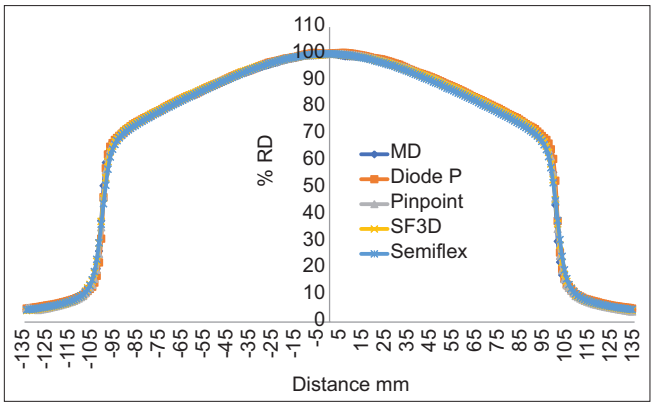

Figure 17: Radial profile curves are shown for 20 cm × 20 cm for different detectors. SF3D: Semiflex 3D, MD: Microdiamond

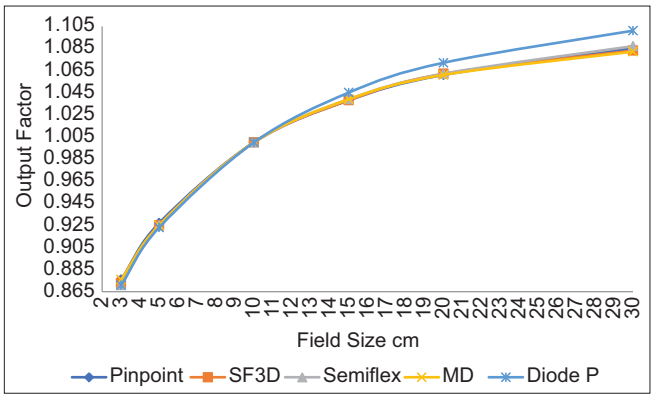

Figure 19: Graphical representation of measured output factor of different detectors. SF3D: Semiflex 3D, MD: Microdiamond

Table 8: Measured output factor comparison

	Output factor				
FS (cm)	Pinpoint	SF3D	Semiflex	MD	Diode P
3	0.876	0.873	0.871	0.876	0.871
5	0.927	0.925	0.925	0.925	0.923
10	1	1	1	1	1
15	1.038	1.038	1.039	1.039	1.045
20	1.061	1.062	1.062	1.061	1.072
30	1.085	1.083	1.087	1.082	1.101

MD: Microdiamond, SF3D: Semiflex 3D, FS: Field size

were more prone to deviation. When very low lateral scatter photons interact at lower depths, the Diode *P* shield material promotes LCPE. This overestimation of ionization results in greater PDD.[28] The data analysis revealed that SF3D is similar with good agreement. All of these measurements were discovered to increase as field sizes grew, indicating that the larger the field size, the more scattered photons interact. This demonstrates that PDD increases when field size increases in SF3D as well.[7] All measures are found to be progressive till 20 cm × 20 cm, then decreasing until 30 cm × 30 cm. Figure 11 shows that the biggest deviation was determined to be 0.8% for 3 cm × 3 cm. In radial profiles, the SF3D chamber has a

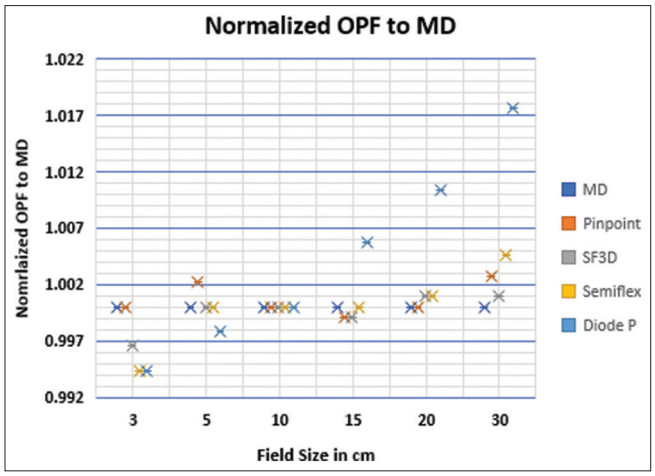

Figure 20: Normalized output factor of different detectors and their variation. SF3D: Semiflex 3D, MD: Microdiamond

greater penumbra for 3 cm × 3 cm than Pinpoint, MD, and Diode P but a smaller penumbra than Semiflex. MD, Diode P, Pinpoint chamber, SF3D, and Semiflex are the effects that emerge in this order. The penumbra of SF3D is in the middle of other detectors. The difference between penumbra and MD is around 1.5 mm (on average). The volume averaging effect of the chamber resulted in higher variance in the Penumbra.[9] The FWHM of the SF3D chamber is comparable to other detectors. The greatest FWHM difference between SF3D and other detectors is <0.5 mm. The measured OPF of SF3D is comparable to other detectors for the relevant field sizes, as shown in the table 8. When compared to MD OPF, the maximum variance for 3 cm × 3 cm is 0.3%. In contrast, Diode P has a higher deviation (2%) at field sizes >10 cm × 10 cm. This is due to the photoelectric property of silicon, which overestimates when it interacts with scattered photons in a large field.[29] Limitation of this study is that the Semiflex 3D detector was not evaluated for 10X FFF photon beam, as the same energy was not available in the linac.

Conclusion

Semiflex 3D chambers perform well in terms of IEC characteristics and relative dosimetry from 3 cm × 3 cm to large field size under 6FFF Beam, according to the conclusions of this experiment. This detector is suitable for OPF measurements in the same field size range as IAEA TRS 483, with no volume averaging correction factor. SF3D was discovered to be highly comparable to MD and superior to standard ionization chambers. Similarly, for large field FFF beam profile analysis according to AERB standard, the SF3D chamber yields comparable radiation field size and penumbra among other radiation detectors used in this study. As a result, the SF3D chamber was shown to be a superior alternative to traditional Semiflex, Pinpoint, and Diode *P* detectors and comparable to a microdiamond detector for relative dosimetry tests ranging from 3 cm × 3 cm to larger field size under 6FFF beam.

Acknowledgment

We acknowledge Mr. Senniyandavar, Mr. KKD Ramesh, Mr. Boopathi, Mr. Jeyaprakash, Mrs. Narmada, Mr. Kalidass, and Mr. Dinakaran for their help and special gratitude and thanks to Mr. B. Viswanathan, Managing Director, PTW Dosimetry India Pvt., Ltd., for lending radiation detectors for this study.

Financial support and sponsorship

Nil.

Conflicts of interest

There are no conflicts of interest.

References

1. Georg D, Knöös T, McClean B. Current status and future perspective of flattening filter free photon beams. Med Phys 2011;38:1280-93.
2. Sharma SD. Unflattened photon beams from the standard flattening filter free accelerators for radiotherapy: Advantages, limitations and challenges. J Med Phys. 2011;36:123-5. doi: 10.4103/0971-6203.83464.
3. Xiao Y, Kry SF, Popple R, Yorke E, Papanikolaou N, Stathakis S, *et al*. Flattening filter-free accelerators: a report from the AAPM Therapy Emerging Technology Assessment Work Group. J Appl Clin Med Phys. 2015;16:5219. doi: 10.1120/jacmp.v16i3.5219.
4. Sudhyadhom A, Kirby N, Faddegon B, Chuang CF. Technical Note: Preferred dosimeter size and associated correction factors in commissioning high dose per pulse, flattening filter free x-ray beams. Med Phys 2016;43:1507-13. doi: 10.1118/1.4941691.
5. Masanga W, Tangboonduangjit P, Khamfongkhruea C, Tannanonta C. Determination of small field output factors in 6 and 10 MV flattening filter free photon beams using various detectors. J Phys 2016. DOI 10.1088/1742-6596/694/1/012027.
6. IEC Medical electrical equipment - Dosimeters with ionization chambers as used in radiotherapy, IEC Guide 60731. Geneva, Switzerland: IEC;2011.
7. Andreo P, Burns DT, Hohlfeld K, Huq M S, Kanai T, Laitano F, *et al*. Absorbed dose determination in external beam radiotherapy: an international code of practice for dosimetry based on standards of absorbed dose to water IAEA Technical Report Series No 398 International Atomic Energy Agency, Vienna 2000.
8. Report No. IEC-60976. Geneva: IEC; International Electrotechnical Commission, Medical electrical equipment - Medical electron accelerators - Functional performance characteristics. 2007.
9. Palmans H, Andreo P, Huq MS, Seuntjens J, Christaki K. Dosimetry of Small Static Fields used in External Beam Radiotherapy: An IAEA–AAPM International Code of Practice for Reference and Relative Dose Determination. Technical Report Series No. 483. Vienna: International Atomic Energy Agency; 2017. Available from: https://www-pub.iaea.org/MTCD/Publications/PDF/D483_web.pdf. [Last accessed on 2023 Sep 02].
10. Griessbach I, Lapp M, Bohsung J, Gademann G, Harder D. Dosimetric characteristics of a new unshielded silicon diode and its application in clinical photon and electron beams. Med Phys. 2005;32:3750-4. doi: 10.1118/1.2124547.
11. Chand B, Kumar M, Kumar M, Priyamvda. Comprehensive Review of Small Field Dosimetry. Eur J Mol Clin Med 2020;7.
12. Brualla-González L, Gómez F, Pombar M, Pardo-Montero J. Dose rate dependence of the PTW 60019 microDiamond detector in high dose-per-pulse pulsed beams. Phys Med Biol. 2016;61:N11-9. doi: 10.1088/0031-9155/61/1/N11. Epub 2015 Dec 1. PMID: 26625177.
13. Reggiori G, Stravato A, Pimpinella M, Lobefalo F, De Coste V, Fogliata A, *et al*. Use of PTW-microDiamond for relative dosimetry of unflattened photon beams. Phys Med 2017;38:45-53.
14. Ralston A, Tyler M, Liu P, McKenzie D, Suchowerska N. Over-response of synthetic microDiamond detectors in small radiation fields. Phys Med Biol. 2014;59:5873-81. doi: 10.1088/0031- 9155/59/19/5873.

15. Ciancaglioni I, Marinelli M, Milani E, Prestopino G, Verona C, Verona-Rinati G, *et al*. Dosimetric characterization of a synthetic single crystal diamond detector in clinical radiation therapy small photon beams. Med Phys. 2012;39:4493-501. doi: 10.1118/1.4729739.
16. The Dosimetry Company. Dosimetry Catolog [Internet]. Freiburg Germany: The Dosimetry Company; 2020. Available from: https://www.ptwdosimetry.com/en/products/semiflex-3d-ion-chamber-31021. [Last accessed on 2023 Sep 02].
17. Momeni Harzanji Z, Larizadeh MH, Namiranian N, Nickfarjam A. Evaluation and Comparison of Dosimetric Characteristics of Semiflex®3D and Microdiamond in Relative Dosimetry under 6 and 15 MV Photon Beams in Small Fields. J Biomed Phys Eng. 2022;12:477-88. doi: 10.31661/jbpe.v0i0.2008-1160.
18. Casar B, Gershkevitsh E, Mendez I, Jurković S, Saiful Huq M. Output correction factors for small static fields in megavoltage photon beams for seven ionization chambers in two orientations - perpendicular and parallel. Med Phys. 2020;47:242-59. doi: 10.1002/mp.13894.
19. Elekta, Elekta InfinityTM, Available from: https://www.elekta.com/products/radiation-therapy/infinity/assets/Infinity-Brochure.pdf. [Last accessed on 2023 Sep 02].
20. The Dosimetry Company. Dosimetry Catolog [Internet]. Freiburg Germany: The Dosimetry Company. Available from: https://www.ptwdosimetry.com/en/radiation-therapy/categories/detectors. [Last accessed on 2023 Sep 02].
21. PTW, MP3-M Water Phantom System (Internet). Available from: https://www.ptwdosimetry.com/en/products/mp3-m-water-phantom-system [Last accessed on 2023 Sep 02].
22. Zope M, Deepali Bhaskar P, Kuriakose A, Aslam PA, George B. Photon Beam Commissioning of Varian Unique Performance Low Energy Linear Accelerator (LINAC). Insights Med Phys 2019;4. doi: 10.21767/2574-285X.100016.
23. Keivan H, Shahbazi-Gahrouei D, Shanei A. Evaluation of dosimetric characteristics of diodes and ionization chambers in small megavoltage photon field dosimetry. Int J Radiat Res 2018;16.
24. Accelerator beam data commissioning equipment and procedures: Report of the TG-106 of the Therapy Physics Committee of the AAPM 2008 American Association of Physicists in Medicine. DOI: 10.1118/1.2969070.
25. Sahani G, Sharma SD, Dash Sharma PK, Deshpande DD, Negi PS, Sathianarayanan VK, *et al.* Acceptance criteria for flattening filter-free photon beam from standard medical electron linear accelerator: AERB task group recommendations J Med Phys. 2014;39:206-11. doi: 10.4103/0971-6203.144482
26. PTW, Beamscan software User Manual; D948.131.00/09. p. 466. available from: https://www.ptwdosimetry.com/en/products/beamscan Last accessed on 2023 Sep 02].
27. Klein EE, Hanley J, Bayouth J, Yin FF, Simon W, Dresser S, *et al*. Task group 142 report: Quality assurance of medical accelerators. Med Phys 2009;36:4197-212.
28. Akino Y, Okamura K, Das IJ, Isohashi F, Seo Y, Tamari K, *et al*. Technical Note: Characteristics of a microSilicon X shielded diode detector for photon beam dosimetry. Med Phys. 2021;48:2004-9. doi: 10.1002/mp.14639.
29. Würfel JU. Dose measurements in small fields. Med Phys Int J. 2013;1:81-90.